Isolation and characterization of a retinal pigment epithelial cell fluorophore: An *all-trans*-retinal dimer conjugate

Nathan E. Fishkin*, Janet R. Sparrow†‡§, Rando Allikmets†‡, and Koji Nakanishi*

Departments of *Chemistry, †Ophthalmology, and ‡Pathology and Cell Biology, Columbia University, New York, NY 10032

Edited by Jeremy Nathans, The Johns Hopkins University School of Medicine, Baltimore, MD, and approved April 5, 2005 (received for review February 14, 2005)

Several lines of investigation suggest that the nondegradable fluorophores that accumulate as lipofuscin in retinal pigment epithelium (RPE) cells contribute to the etiology of macular degeneration. Despite evidence that much of this fluorescent material may originate as inadvertent products of the retinoid cycle, the enzymatic pathway by which the 11-*cis*-retinal chromophore of rhodopsin is generated, the only fluorophores of the RPE to be characterized as yet have been A2E and its isomers. Here, we report the isolation and structural characterization of an additional RPE lipofuscin fluorophore that originates as a condensation product of two molecules of *all-trans*-retinal (ATR) dimer and forms a protonated Schiff base conjugate with phosphatidylethanolamine (PE), the latter conjugate (ATR dimer–PE) having UV-visible absorbance maxima at 285 and 506 nm. ATR dimer was found to form natively in bleached rod outer segments *in vitro* and when rod outer segments were incubated with ATR. HPLC analysis of eyecups that included RPE and isolated neural retina from *Abcr* −/− mice and RPE isolated from human donor eyes revealed the presence of a pigment with the same UV-visible absorbance and retention time as synthetic ATR dimer–PE conjugate. Evidence that ATR dimer undergoes a photooxidation process involving the addition of oxygens at double bonds as well as an aromatic demethylation also may indicate a role for this molecule, or its derivatives, in the photoreactivity of RPE lipofuscin.

phosphatidylethanolamine | lipofuscin | retinal pigment epithelium | macular degeneration | ABCA4

Whereas the lipofuscin that is amassed by most nonproliferating cells is derived from autophagy (1), lipofuscin fluorophores of the retinal pigment epithelium (RPE) originate, in large part, from photoreceptor cells (2), with >90% of the fluorescent material being generated from conjugates formed by retinoids of the visual cycle (3, 4). RPE lipofuscin fluorophores accumulate with age (5, 6), the greatest accretion is in RPE cells underlying the central retina (6), and the retinoid-derived fluorophores are particularly abundant in Stargardt's disease (7, 8), a macular degeneration of juvenile onset. Indeed, several lines of evidence indicate that the lipofuscin fluorophores that accumulate in RPE contribute to the death of these cells in some forms of macular degeneration (5, 9–13). The loss of RPE is a critical event because it is thought that it leads to bystander-like degeneration of photoreceptors that culminates in visual impairment.

As yet, the only RPE lipofuscin fluorophores that have been characterized are A2E, its 13-(*Z*)-double-bond isomer iso-A2E, and other minor *Z*-isomers of A2E (14–19). These compounds are generated by hydrolysis of the phosphate ester of A2-PE, the phosphatidyl-pyridinium bisretinoid precursor that forms in rod outer segments (ROS). The synthesis of A2-PE occurs when molecules of *all-trans*-retinal (ATR), instead of undergoing reduction to *all-trans*-retinol, form conjugates with phosphatidylethanolamine (PE) through a series of random/nonenzyme-mediated reactions (16, 19). This pyridinium bisretinoid pathway is more active under conditions of elevated concentrations of ATR, circumstances that likely include dysfunction of the ABCA4 (ABCR) transporter, the latter being the protein product of the Stargardt's disease gene (20). Other modulations of pyridinium bisretinoid pathway are levels of illumination (17, 18, 21) and the kinetics of the retinoid cycle (22).

Since A2E was characterized (14, 15), several consequences of its accumulation have been reported. Because of its amphiphilic properties, A2E can exert detergent-like effects on cell membranes (23–26), perturb lysosomal function (27, 28), and mediate blue-light damage (29–31). Blue-light irradiation of A2E leads to the photooxidation of A2E such that oxygens are added to carbon–carbon double bonds along the side arms of the molecule (32, 33). The question still remains, however, as to whether other retinoid-derived fluorescent compounds accumulate in RPE in addition to A2E and its isomers. In this regard, we recently reported that, at elevated ATR concentrations, a fluorescent bisretinoid adduct can form on lysine residues of rhodopsin (A2-Rh) in ROS (34). These findings may signify that fluorescent peptide fragments bearing bisretinoid moieties become deposited in RPE cells. Additionally, we now report the formation of an enantiomerically enriched ATR dimer–PE conjugate. We propose that conditions can exist in the outer segment whereby, upon release of ATR from opsin, the formation of this bischromophore begins with the generation of ATR dimer, a condensation product of two molecules of ATR. Subsequent reaction of ATR dimer with PE generates the Schiff base (SB) conjugate that accumulates in RPE cells.

Materials and Methods

Tissue Processing, Extraction, and HPLC Analysis. Bovine photoreceptor ROS were isolated as described (34) and incubated with 50 μM ATR (34) in the dark for 3 days at 37°C. Alternatively, to release endogenous ATR, ROS were exposed to white light under conditions described in ref. 17. *Abcr*-null mutant mice (129/SV × C57BL/6J) were generated, genotyped, and housed as reported in ref. 22. Posterior eye poles were dissected, and tissues were collected as either eyecups including sclera, choroid, and RPE (RPE-eyecups) or isolated neural retina. Chloroform/methanol (2:1 $CHCl_3$/MeOH) extracts (16, 22) of the tissues were concentrated *in vacuo* and redissolved in 100 μl of hexane. Components were immediately separated on a YMC-Pack silica column [silica 5-μm, 150 × 4.5 mm, mobile phase hexanes/2-propanol/ethanol/phosphate-buffered saline (pH 7.0)/acetic acid 485:376:100:20:0.275; flow rate, 0.75 ml/min; detection, 500 nm; YMC, Kyoto]. A photodiode array detector was used to monitor the UV spectrum of each eluted compound. Reverse-

This paper was submitted directly (Track II) to the PNAS office.

Abbreviations: ATR, *all-trans*-retinal; PE, phosphatidylethanolamine; ROS, rod outer segments; RPE, retinal pigment epithelium; SB, Schiff base; PSB, protonated SB.

§To whom correspondence should be addressed. E-mail: jrs88@columbia.edu.

phase HPLC (C_4 column 250 × 4 mm; gradient, 0–5 min; 85–100% acetonitrile/water; 5–30 min, 100% acetonitrile; flow rate, 1.5 ml/min; 450-nm monitoring) also was performed on the extracts of six pooled human eyes (age 31–40 years; National Disease Research Interchange, Philadelphia). The extract was concentrated and redissolved in 100 μl of methylene chloride before injection.

Synthesis of ATR Dimer, ATR Dimer–PE Conjugate, and ATR Dimer–Ethanolamine Conjugate. ATR dimer was synthesized by treating ATR with 1 eq of sodium hydride (NaH) in dry tetrahydrofuran (35). To synthesize the conjugates, 50 mg of racemic ATR dimer was dissolved in 2 ml of a 10:5:1 $CHCl_3$/MeOH/Et_3N solution and added to a 10-ml round-bottom flask containing 4-Å molecular sieves. The solution was cooled to 0°C, and 5 molar equivalents of either ethanolamine (Sigma-Aldrich) or dipalmitoyl (C16:0) L-α-PE (Sigma-Aldrich) was added in 1 ml of chloroform dropwise over 10 min. The reaction was allowed to proceed for 2 h, at which time the solvents were evaporated. ATR dimer–ethanolamine conjugate was purified by using SiO_2 chromatography (1:1 EtOAc/hexanes), and ATR dimer–PE conjugate was subjected to preparative HPLC [Vydac C_{18}, 20% H_2O → 100% CH_3CN (0.1% trifluoracetic acid), 4 ml/min, 500-nm detection].

^{1}H NMR of ATR Dimer–SB Conjugate. ($CDCl_3$, 500 MHz): δ 7.95 (s, 1 H, CH═N), 6.95 (dd, J = 7.5 Hz, J = 14 Hz, 1 H, H11), 6.7 (d, J = 6.1 Hz, 1 H, H15), 6.48 (d, J = 15 Hz, 1 H, H12), 6.3–6.0 (m, 8 H, H11′, H7, H10, H8, H14, H7′, H8′, H10′), 5.9 (d, J = 15.4 Hz, 1 H, H12′), 3.8 (t, J = 5.6 Hz, 2 H, N–C**H**$_2$), 3.65 (t, J = 5.6 Hz, 2 H, N–CH_2–C**H**$_2$–OH), 2.7 (d, J = 16.6 Hz, 1 H, equatorial H20), 2.45 (d, J = 16.6 Hz, 1 H, axial H20), 2.06 (m, 7 H, H4, H19, H4′), 1.9 (s, 3 H, H19′), 1.75 (s, 3 H, H18), 1.71 (s, 3 H, H18′), 1.68 (m, 4 H, H3, H3′), 1.51 (m, 4 H, H2, H2′), 1.45 (s, 3 H, H20′), 1.07 (s, 6 H, H16, H17), 1.03 (s, 6H, H16′, H17′). Fast atom bombardment MS $(M)^+$ = 594.6.

Photooxidation of ATR Dimer–PE Conjugate. A 100 μM solution of the ATR dimer in H_2O (pH 7, 0.5% DMSO) or $CHCl_3$ was irradiated with blue light (60-W lamp, 10 cm, blue band-pass filter 400–440 nm) at 25°C for the times indicated.

Results

In addition to the fluorescent protein adduct A2-Rh (34), a fluorophore was isolated in ROS under conditions similar to those previously shown to result in the formation of A2-PE, an A2E precursor (17, 19). Specifically, after isolated bovine ROS were incubated with ATR, reverse-phase HPLC revealed a previously unidentified species with peak shape, UV profile (λ_{max} = 295 and 432 nm), and retention time (RT = 6.95 min) identical to those of the compound generated by using the method of Verdegem *et al.* (35), for base-catalyzed (NaH) condensation of two molecules of ATR (Fig. 1). This pigment (35, 36), which will be referred to as ATR dimer, also exhibited a UV-visible spectrum and retention time that was distinctly different from A2-PE (RT = 13–15 min; λ_{max} = 338 and 446 nm) (Fig. 1). By using atmospheric pressure chemical ionization MS, the molecular mass (551.9 m/z, M + H) of the isolate also was found to be the same as that of the ATR dimer. ^{1}H NMR (Fig. 2) further revealed that the isolated compound had a spectrum identical to the synthetic racemic sample of ATR dimer. The same compound also was identified in isolated ROS illuminated to induce photoisomerization and release of endogenous ATR, but, compared with A2-PE, it was present at a much lower amount (Fig. 1).

Recognizing the possibility that the ATR dimer would form a SB conjugate with amines *in vivo*, we incubated the synthetic racemic sample of ATR with dipalmitoyl (C16:0) L-α-PE in

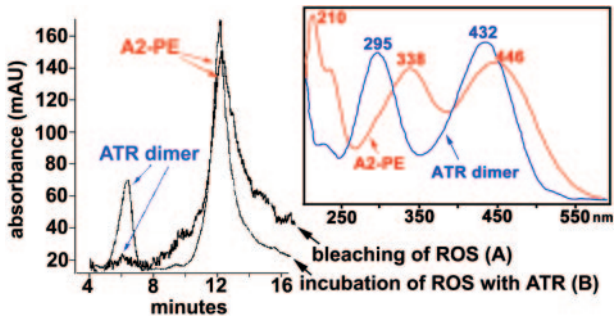

Fig. 1. Reverse-phase HPLC profile of extracts of bovine ROS that had been bleached to release endogenous ATR (trace A) or that had been incubated with exogenous ATR (trace B). Absorbance was detected at 450 nm. A2-PE and ATR dimer were identified by coinjection of synthetic samples of these pigments. (*Upper Right*) UV-visible spectra of A2-PE and ATR dimer in acetonitrile/water are shown.

10:5:1 $CHCl_3$/MeOH/Et_3N to generate ATR dimer–PE conjugate (Fig. 3). The latter compound had a UV spectrum exhibiting two peaks at λ_{max} 285 and 506 nm when eluted on a normal-phase HPLC column (0.1% acetic acid). The dramatic ≈70-nm red shift in the long-wavelength band of ATR dimer–PE conjugate, compared with ATR dimer, is consistent with the formation of a protonated SB (PSB). Because a SB is a chemically labile bond, we also supposed that under strong acidic conditions, ATR dimer–PE conjugate could decompose or be converted to other compounds. To test this possibility, we reacted ATR with ethanolamine to generate an ATR dimer–ethanolamine conjugate (Fig. 4). Ethanolamine, instead of PE, was used as the reactant in these experiments because the ATR dimer–ethanolamine conjugate is a simpler system; in addition, because condensation of ethanolamine with ATR is more facile, it afforded more reaction product. Subsequent treatment of the ATR dimer–ethanolamine conjugate with HCl (100 mM) in hexane, acid conditions that would not exist physiologically, generated A2E overnight (Fig. 4). The mechanism for this transformation could involve an initial acid-catalyzed retroaldol process to open the cyclohexadiene, followed by ring reclosure to give the more stable A2E.

Because the levels of A2E have been shown to be considerably increased in *Abcr*-null mutant mice (18, 22, 37, 38), presumably because of inadequate clearance of ATR from the outer segment, we next sought evidence of the presence of the ATR dimer or its conjugates in extracts of RPE eyecups and neural retina

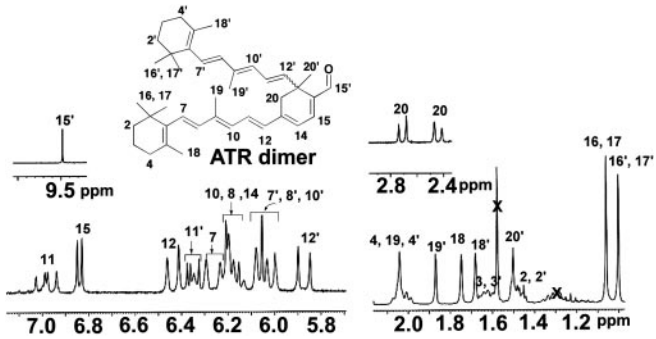

Fig. 2. ^{1}H NMR spectrum (400 MHz; $CDCl_3$) of the pigment in ATR-treated ROS that was isolated by using reverse-phase HPLC at a retention time of 6.95 min. Two sets of *gem*-dimethyl peaks on C1 and C1′ were immediately suggestive of a dimerized retinal product and verified the structure as that of ATR dimer. The peaks are assigned based on the numbering shown with the structure. X, solvent impurities.

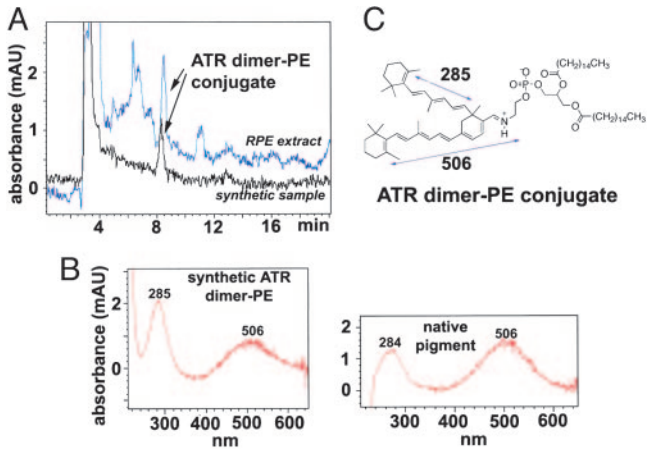

Fig. 3. Formation of an ATR dimer–PE conjugate. (*A*) Normal-phase HPLC (0.1% AcOH buffer, 500-nm detection) profiles of synthetic ATR dimer–PE conjugate (synthetic sample) and a pigment extracted from RPE eyecups of *Abcr* −/− mice (RPE extract). mAU, milliabsorbance unit. (*B*) UV-visible spectra of synthetic ATR dimer–PE conjugate (*Left*) and the native 506-nm pigment isolated from *Abcr* −/− mice (*Right*). (*C*) Structure of ATR dimer–PE conjugate. The absorbance spectrum of this pigment is due to 295- and 506-nm chromophores.

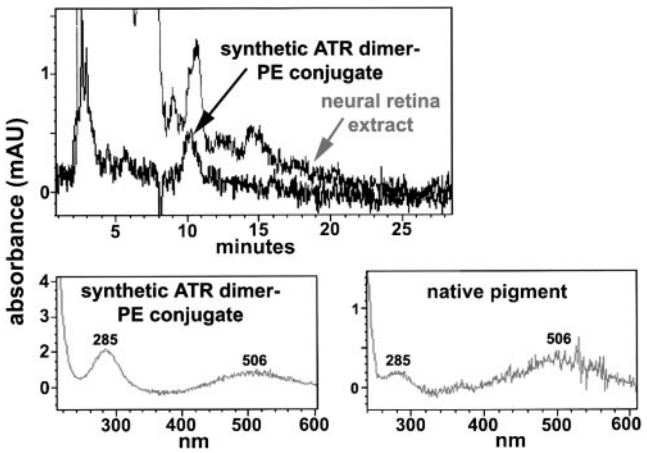

Fig. 5. Identification of ATR dimer–PE conjugate in neural retina. (*Upper*) Normal-phase HPLC of synthetic ATR dimer–PE conjugate and chloroform/methanol extract of neural retina from *Abcr* −/− mice. (*Lower*) UV-visible spectra of synthetic ATR dimer–PE conjugate (*Left*; retention time, 10.6 min) and corresponding native pigment from neural retina (*Right*; retention time, 10.6 min).

obtained from these mice. To confirm the phenotype of these mutant mice, eyecups were obtained from 3-month-old mice raised under 12-hour cyclic lighting, and A2E was quantified by using HPLC. The levels were found to be 20-fold higher in *Abcr* −/− mice, compared with wild-type mice (data not shown), a difference similar to that reported in refs. 18, 22, and 37. Subsequent normal-phase HPLC analysis of extracts from RPE eyecups of *Abcr* −/− mice (Fig. 3) and neural retinae from *Abcr* −/− mice (Fig. 5) with monitoring at 500 nm revealed the presence of a peak with UV and retention time consistent with that of the ATR dimer–PE conjugate. In comparable samples of wild-type mice, this 506-nm species was not detectable (data not shown). The naturally occurring 506-nm pigment appeared to have a phospholipid moiety composed of at least four different fatty acyl chains as determined by MALDI-TOF MS (data not shown). As expected for a SB conjugate, raising the pH of the eluent solvent above 7.5 dramatically blue shifted the long-wavelength band of the UV spectrum of synthetic ATR dimer–PE conjugate (Fig. 6); the compound isolated from eyecups of *Abcr* mice responded similarly (data not shown). The pH dependence of the absorption spectrum reflects the deprotonation of the SB in ATR dimer–PE conjugate with equilibrium being reached between PSB and SB.

Because it has been shown previously that A2E can readily be resolved in the HPLC profile of extracted RPE from 5% of a single human eye (16), it seemed reasonable to expect that the ATR dimer–PE conjugate or related pigments also could be detected. Thus, RPE cells were isolated from individual human eyes from donors 31–40 years old. With monitoring at 500 nm, a series of peaks representing pigments that are considerably less polar than A2E and iso-A2E were detected with retention times ranging from 15 to 20 min. The UV spectra obtained by photodiode array detection revealed that the fraction at 15.5 min contained two peaks with λ_{max} at 270 and 504 nm, whereas the pigment at 18.6 min had peaks with λ_{max} 264 and 500 nm. A peak at 17.6 min had UV maxima at 279 and 485 nm (Fig. 7). The range of retention times observed may reflect the varied fatty acid composition of the PE constituent.

We also were interested to know whether ATR dimer–PE conjugate undergoes photooxidation, as does A2E. Because the polyene structure susceptible to oxidation resides in the ATR dimer portion of the ATR dimer–PE conjugate, a sample of ATR dimer in H_2O (0.1% DMSO) was irradiated (400–440 nm). Subsequent fast atom bombardment MS analysis showed two major molecular ion peaks at m/z 647.7 and 663.7 (Fig. 8). The mass of each of these species was higher than that of ATR dimer (551.9). The m/z 647.7 could be attributed to the addition of 6 oxygen atoms, whereas the m/z 663.7 peak corresponded to an apparent addition of 7 oxygen atoms to the ATR dimer. After blue-light irradiation of ATR dimer in $CDCl_3$, ^1H NMR analysis revealed new resonances at δ = 7.77, 7.94, 8.04, and 11.7δ that were consistent with the presence of an aldehyde next to an aryl ring and were indicative of an aromatization of the central

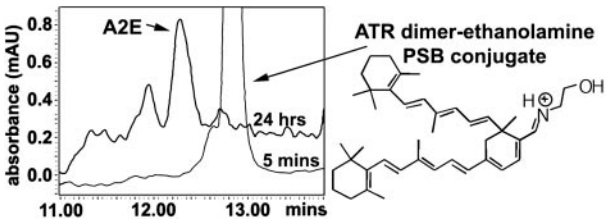

Fig. 4. Reverse-phase HPLC profile of ATR dimer–ethanolamine 5 min after exposure to 100 mM HCl and again 24 h later. The peak corresponding to ATR dimer–ethanolamine conjugate was depleted and replaced by a peak with a retention time and UV spectrum consistent with A2E.

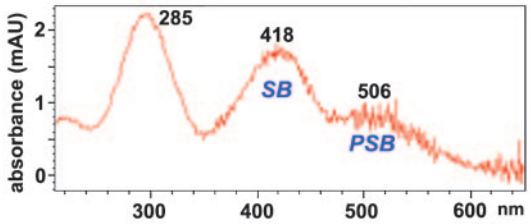

Fig. 6. The SB nitrogen in ATR dimer–PE conjugate is protonated. The UV-visible spectrum of native 506-nm pigment isolated from eyecups of *Abcr* −/− mice and analyzed by normal-phase HPLC without acetic acid buffer is shown. Raising the pH leads to the appearance of an additional peak at 418 nm due to deprotonation of the SB. The presence of both the 418- and 506-nm peaks indicates an equilibrium between the SB and PSB forms of the pigment.

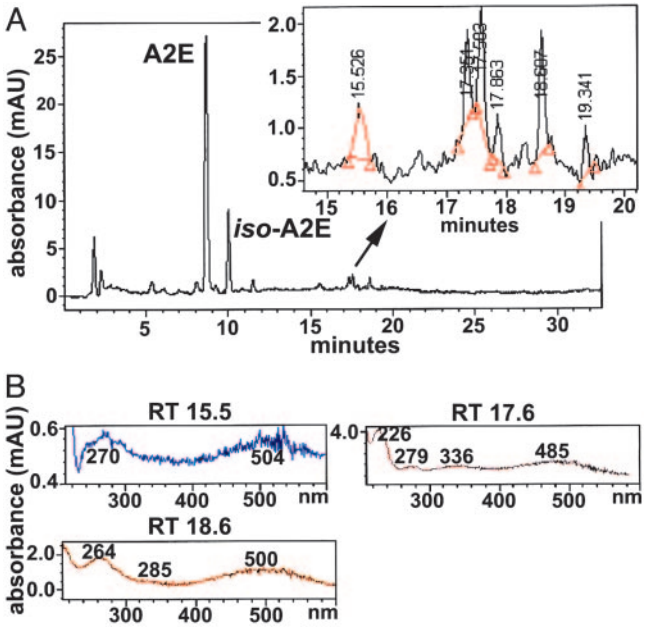

Fig. 7. Detection of ATR dimer–PE conjugate in human RPE cells. (*A*) Reverse-phase HPLC analysis of extracts of isolated RPE pooled from six human eyes. Monitoring was at 500 nm. (*B*) UV-visible spectra of peaks at retention times (RT) 15.5, 17.6, and 18.6 min exhibit absorbances centered at 500 nm.

cyclohexadiene core (Fig. 9). The bleaching behavior of ATR dimer also is demonstrated spectrophotometrically (Fig. 8*C*). Thus, when blue-light irradiation was carried out in aqueous media by using successive 10-sec exposures with measurements 30 sec after each bleach, decreases in absorbance at 290 and 430 nm were observed. The combined UV and NMR data of the photodecomposition products of the ATR dimer suggest that the

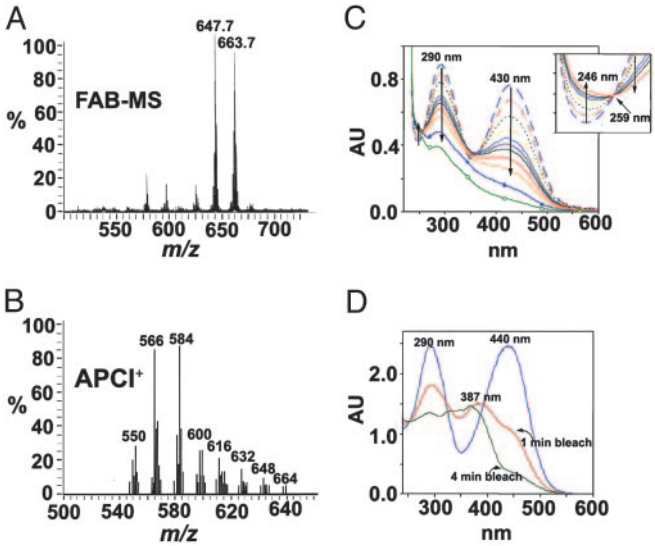

Fig. 8. Bleaching behavior of ATR dimer in chloroform and water. ATR dimer (100 μM) in water (*A* and *C*) or chloroform (*B* and *D*) was exposed to 2 min of blue light (430 nm, 60 W, 10 cm) and then analyzed by using MS (*A* and *B*). FAB, fast atom bombardment; APCI, atmospheric pressure chemical ionization. UV-visible spectra (*C* and *D*) were obtained after successive 10-sec bleaches in water (*C*) and after the indicated bleaching times in chloroform (*D*). *C Inset* shows an isosbestic point at 259 nm and a corresponding increase in absorption at 246 nm, which is consistent with the main charge transfer band of benzaldehyde. Arrows indicate the trends in absorbance change.

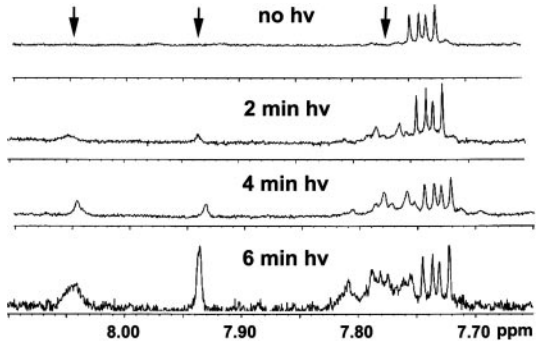

Fig. 9. ^{1}H NMR analysis of irradiated ATR dimer. ATR dimer was either unirradiated (no $h\nu$) or irradiated for 2, 4, or 6 min (430 nm, 0.19 mW/mm^2). The presence of aromatic protons (arrows) upon blue-light exposure suggests aromatization of the central hexadiene core.

structure of the m/z 663.7 species may be that of a polyoxygenated species corresponding to the addition of 8 oxygen atoms to the polyene side arms as well as an aromatic demethylation that formally removes 16 mass units. The bleaching behavior of the ATR dimer in $CHCl_3$ also was examined after 1- and 4-min exposures (Fig. 8*D*). Atmospheric pressure chemical ionization MS demonstrated the formation of several higher-molecular-mass adducts differing by 16 mass units; the highest m/z species at 664 likely corresponds to a octa-oxygenated species (Fig. 8*B*). That the ATR dimer bleaches less efficiently in $CHCl_3$ can be seen by comparing the UV spectra in Fig. 8 *C* and *D*. This difference also is reflected in the mass spectrum (Fig. 8*B*), which shows a relatively large population of the monooxygenated and dioxygenated species with fewer higher-order adducts. Irradiation of an ATR dimer–ethanolamine conjugate also resulted in the addition of 3–4 oxygen atoms as determined by fast atom bombardment MS (data not shown).

It is worth noting that the ATR dimer does not seem to form synthetically in solution under ostensibly neutral conditions. Proline, which is known to catalyze condensations of this type, reacted with ATR to produce a SB only in ethanol. It was found that addition of a base such as triethylamine or diisopropylethylamine was needed to produce any dimerized product. Because ATR dimer possesses a stereogenic center at C13′, and its formation in photoreceptors is likely the result of general acid–base catalysis by membrane-bound proteins in the outer segment, the possible enantiomeric excess of this isolated retinoid was investigated and found to favor the 13′ (*R*) configuration with a 13% enantiomeric excess (39). This enantioenrichment is consistent with the involvement of a chiral protein environment in the catalysis.

Discussion

We have isolated and structurally characterized ATR dimer–PE conjugate, an RPE lipofuscin fluorophore. Based on the experiments with isolated ROS, we suggest that synthesis of this chromophore begins in the outer segment membrane with the formation of ATR dimer, a condensation product of two molecules of ATR. Evidence also is provided that ATR dimer readily forms a SB conjugate with PE, although reactions between the aldehyde group of ATR dimer and other amines also may occur. The ATR dimer–PE conjugate exhibits a red-shifted UV-visible spectrum, and its UV profile and HPLC retention time are the same as a pigment isolated from extracts obtained from RPE eyecups and neural retinae of *Abcr*-null mutant mice. Pigments with UV-visible absorbances corresponding to that of ATR dimer–PE conjugate also were detected in RPE isolated from human eyes. *In vitro* studies showed that only a trace amount of

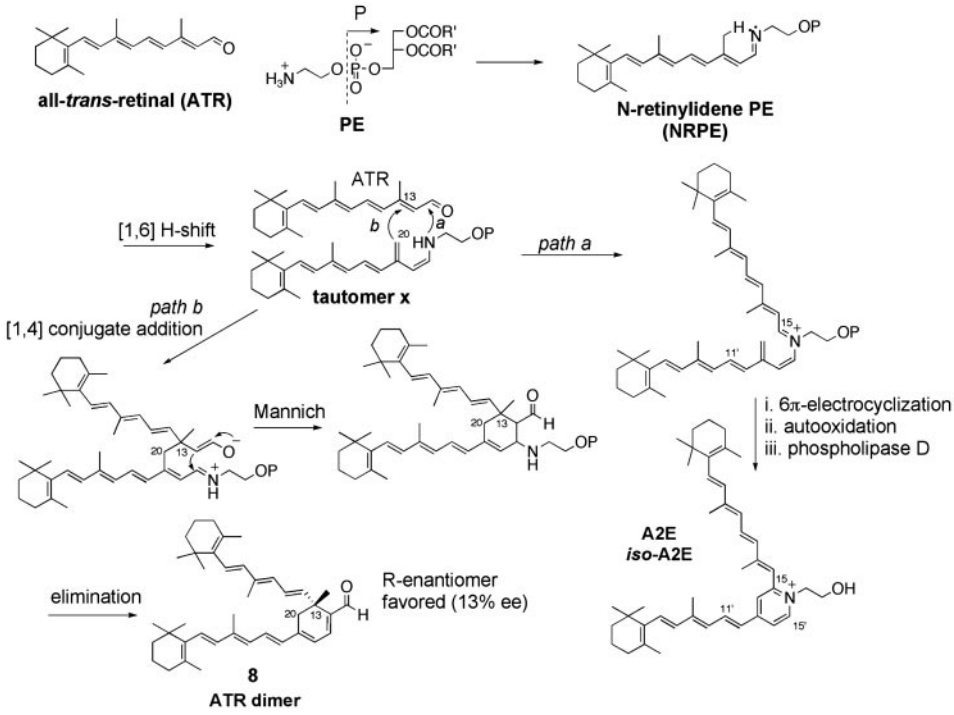

Fig. 10. Proposed biosynthetic pathway of ATR dimer and A2E. ATR that is released from opsin upon photoisomerization of 11-*cis*-retinal reacts with PE to produce the *N*-retinyl-phosphatidylethanolamine (NRPE) SB. Both ATR dimer and A2-PE may form from the same tautomer *x* arising from a [1,6] H-shift of NRPE (15). Tautomer *x* can form an iminium ion with a second ATR according to path a, and after 6 π-aza electrocyclization and autooxidation, A2-PE is formed. Conversely, in path b, C20 of NRPE reacts with C13 of free ATR in a Michael-type addition, followed by a Mannich reaction to close the ring, and elimination of the amino group of PE, yielding the ATR dimer.

ATR dimer is formed under conditions of release of endogenous retinal from opsin, yet a much larger amount is produced relative to A2-PE at elevated levels of ATR. This observation is consistent with the finding that in wild-type mice, the 506-nm pigment does not reach detectable levels, whereas the pigment is readily demonstrable in *Abcr*-knockout mice. Because this 506-nm pigment is found in both neural retina, samples of which included ROS, and RPE cells, it seems reasonable that ATR dimer forms a conjugate with PE in the outer segment and that the resulting pigment then becomes deposited in RPE cells through photoreceptor outer segment disk phagocytosis. Like A2E, the polyene arms of the ATR dimer–conjugate are capable of forming polyoxygenated adducts when irradiated with short-wavelength visible light. It will be of interest to determine whether these photoadducts form consequent to the photosensitization of ATR dimer.

Base-catalyzed condensation of α,β-unsaturated aldehydes containing a β-methyl substituent have been previously reported to produce cyclohexa-1,3-diene-carbaldehydes similar to ATR dimer. Based on the reported mechanism for this type of transformation (40, 41), a pathway for biogenesis of ATR dimer is proposed in Fig. 10. Within the context of this postulated scheme, ATR dimer could form in outer segments under ostensibly neutral conditions with ATR dimer and A2-PE, the precursor of A2E, both forming from the same tautomer that was previously hypothesized to arise from a [1,6] H-shift of *N*-retinyl-phosphatidylethanolamine (NRPE) (15). Indeed, that ATR dimer forms in ROS lends support to the proposed existence of this tautomer, as this intermediate would account for the nucleophilicity of C20 and its participation in the [1,4] conjugate addition. According to the scheme in Fig. 10, C20 of NRPE would react with C13 of free ATR in a Michael-type addition, and after ring closure and elimination of the amino group of PE, ATR dimer would be formed. It should be noted, however, that it is not known whether ATR is released in a free form after decay of metarhodopsin II (42). Evidence that the ATR dimer–PE conjugate is readily detectable in the *Abcr* $-/-$ mouse suggests that path b in this proposed biosynthetic scheme (Fig. 10) would be more active at elevated ATR concentrations. ATR dimer can be expected to react with amines through its aldehyde group, and indeed, we have shown that ATR dimer forms a PSB conjugate with PE. Previous reports of an $\approx$500-nm species detected in ROS and RPE cells of *Abcr* $-/-$ mice (18, 38, 43) identified this pigment as A2PE-H_2, a dihydropyridinium molecule that has been proposed as an intermediate in the A2E biosynthetic pathway (16). However, several lines of reasoning suggested that the 500-nm pigment isolated by Mata *et al.* was not A2-PE-H_2. For instance, A2PE-H_2 can be expected to be an unstable intermediate that undergoes facile autooxidation. The presence of two hydrogens in the pyridinium ring also is not consistent with an $\approx$54-nm red shift in the UV absorbance (A2PE-H_2 relative to A2-PE). Additionally, incubation of A2PE-H_2 in acid would not be expected to promote aromatization to A2E (18). The structural analysis reported here confirms that the 500-nm pigment that we have detected in eyecups of *Abcr* $-/-$ mice and in human RPE is ATR dimer–PE conjugate. The observation that the ATR dimer–ethanolamine conjugate rearranges to A2E under strong acidic conditions is of interest because this behavior was also reported for the 500-nm pigment described by Mata *et al.* (18, 38, 43). Whether these pigments are the same, however, awaits clarification. It should be noted that although ATR dimer–ethanolamine conjugate was converted to A2E within 24 h when incubated with 100 mM HCl, this level of acidity (pH $\approx$ 1) would not be reached in the lysosomes of the RPE cell within which these fluorophores accumulate. On the other hand, one cannot rule out the possibility that under *in vivo* conditions, a slow rearrangement to A2E could occur.

The lipofuscin of RPE cells likely consists of a mixture of fluorophores, only some of which have been identified. The concept that retinoid-derived conjugates consitute a substantial portion of this material is supported by reports that RPE lipofuscin is profoundly reduced in animals lacking the 11-*cis* and ATR chromophores because of either dietary deficiency or gene knockout (3, 4, 44). Spectrophotometric studies of RPE lipofuscin have generally reported excitation spectra that are broader than that of the bisretinoid fluorophore A2E, with the excitation maximum of A2E occurring at slightly shorter wavelengths (45). The presence of ATR dimer conjugates in the lipofuscin mixture may account for the spectral differences between A2E and that of whole lipofuscin. Similarly, although A2E is the most studied of the lipofuscin fluorophores, it is not expected to be the only photosensitizer in RPE lipofuscin. Because the lipofuscin of RPE is considered to be responsible for the sensitivity of the cell to blue-light damage (46–49), it will be important to determine the extent to which ATR dimer–PE conjugate contributes to the photoreactivity of RPE lipofuscin.

This work was supported by National Institutes of Health Grants EY12951 (to J.R.S.), GM34509 (to K.N.), and EY13435 (to R.A.); National Institutes of Health Vision Training Grant EY139933 (to N.E.F.); and the Macula Vision Research Foundation (to J.R.S.).

1. Cuervo, A. M. & Dice, J. R. (2000) *Exp. Gerontol.* **35,** 119–131.
2. Katz, M. L., Drea, C. M., Eldred, G. E., Hess, H. H. & Robison, W. G., Jr. (1986) *Exp. Eye. Res*. **43,** 561–573.
3. Katz, M. L., Drea, C. M. & Robison, W. G., Jr. (1986) *Mech. Ageing Dev.* **35,** 291–305.
4. Katz, M. L. & Redmond, T. M. (2001) *Invest. Ophthalmol. Visual Sci.* **42,** 3023–3030.
5. Wing, G. L., Blanchard, G. C. & Weiter, J. J. (1978) *Invest. Ophthalmol. Visual Sci.* **17,** 601–607.
6. Delori, F. C., Goger, D. G. & Dorey, C. K. (2001) *Invest. Ophthalmol. Visual Sci.* **42,** 1855–1866.
7. Delori, F. C., Staurenghi, G., Arend, O., Dorey, C. K., Goger, D. G. & Weiter, J. J. (1995) *Invest. Ophthalmol. Visual Sci.* **36,** 2327–2331.
8. von Ruckmann, A., Fitzke, F. W. & Bird, A. C. (1997) *Arch. Ophthalmol.* **115,** 609–615.
9. Dorey, C. K., Wu, G., Ebenstein, D., Garsd, A. & Weiter, J. J. (1989) *Invest. Ophthalmol. Visual Sci.* **30,** 1691–1699.
10. Feeney-Burns, L., Hilderbrand, E. S. & Eldridge, S. (1984) *Invest. Ophthalmol. Visual Sci.* **25,** 195–200.
11. von Ruckmann, A., Fitzke, F. W. & Bird, A. C. (1999) *Graefes Arch. Clin. Exp. Ophthalmol.* **237,** 1–9.
12. Holz, F. G., Bellman, C., Staudt, S., Schutt, F. & Volcker, H. E. (2001) *Invest. Ophthalmol. Visual Sci.* **42,** 1051–1056.
13. Holz, F. G., Bellmann, C., Margaritidis, M., Schutt, F., Otto, T. P. & Volcker, H. E. (1999) *Graefes Arch. Clin. Exp. Ophthalmol.* **237,** 145–152.
14. Eldred, G. E. & Lasky, M. R. (1993) *Nature* **361,** 724–726.
15. Sakai, N., Decatur, J., Nakanishi, K. & Eldred, G. E. (1996) *J. Am. Chem. Soc.* **118,** 1559–1560.
16. Parish, C. A., Hashimoto, M., Nakanishi, K., Dillon, J. & Sparrow, J. R. (1998) *Proc. Natl. Acad. Sci. USA* **95,** 14609–14613.
17. Ben-Shabat, S., Parish, C. A., Vollmer, H. R., Itagaki, Y., Fishkin, N., Nakanishi, K. & Sparrow, J. R. (2002) *J. Biol. Chem.* **277,** 7183–7190.
18. Mata, N. L., Weng, J. & Travis, G. H. (2000) *Proc. Natl. Acad. Sci. USA* **97,** 7154–7159.
19. Liu, J., Itagaki, Y., Ben-Shabat, S., Nakanishi, K. & Sparrow, J. R. (2000) *J. Biol. Chem.* **275,** 29354–29360.
20. Allikmets, R., Shroyer, N. F., Singh, N., Seddon, J. M., Lewis, R. A., Bernstein, P. S., Peiffer, A., Zabriskie, N. A., Li, Y., Hutchinson, A., *et al.* (1997) *Science* **277,** 1805–1807.
21. Radu, R. A., Mata, N. L., Bagla, A. & Travis, G. H. (2004) *Proc. Natl. Acad. Sci. USA* **101,** 5928–5933.
22. Kim, S. R., Fishkin, N., Kong, J., Nakanishi, K., Allikmets, R. & Sparrow, J. R. (2004) *Proc. Natl. Acad. Sci. USA* **101,** 11668–11672.
23. Sparrow, J. R., Parish, C. A., Hashimoto, M. & Nakanishi, K. (1999) *Invest. Ophthalmol. Visual Sci.* **40,** 2988–2995.
24. Sparrow, J. R., Fishkin, N., Zhou, J., Cai, B., Jang, Y. P., Krane, S., Itagaki, Y. & Nakanishi, K. (2003) *Vision Res.* **43,** 2983–2990.
25. De, S. & Sakmar, T. P. (2002) *J. Gen. Physiol.* **120,** 147–157.
26. Suter, M., Reme, C. E., Grimm, C., Wenzel, A., Jaattela, M., Esser, P., Kociok, N., Leist, M. & Richter, C. (2000) *J. Biol. Chem.* **275,** 39625–39630.
27. Finneman, S. C., Leung, L. W. & Rodriguez-Boulan, E. (2002) *Proc. Natl. Acad. Sci. USA* **99,** 3842–3847.
28. Holz, F. G., Schutt, F., Kopitz, J., Eldred, G. E., Kruse, F. E., Volcker, H. E. & Cantz, M. (1999) *Invest. Ophthalmol. Visual Sci.* **40,** 737–743.
29. Sparrow, J. R., Nakanishi, K. & Parish, C. A. (2000) *Invest. Ophthalmol. Visual Sci.* **41,** 1981–1989.
30. Schutt, F., Davies, S., Kopitz, J., Holz, F. G. & Boulton, M. E. (2000) *Invest. Ophthalmol. Visual Sci.* **41,** 2303–2308.
31. Sparrow, J. R. & Cai, B. (2001) *Invest. Ophthalmol. Visual Sci.* **42,** 1356–1362.
32. Sparrow, J. R., Zhou, J., Ben-Shabat, S., Vollmer, H., Itagaki, Y. & Nakanishi, K. (2002) *Invest. Ophthalmol. Visual Sci.* **43,** 1222–1227.
33. Ben-Shabat, S., Itagaki, Y., Jockusch, S., Sparrow, J. R., Turro, N. J. & Nakanishi, K. (2002) *Angew. Chem. Int. Ed.* **41,** 814–817.
34. Fishkin, N., Jang, Y. P., Itagaki, Y., Sparrow, J. R. & Nakanishi, K. (2003) *Org. Biomol. Chem.* **1,** 1101–1105.
35. Verdegem, P. J. E., Monnee, M. C. F., Mulder, P. P. J. & Lugtenburg, J. (1997) *Tetrahedron Lett.* **38,** 5355–5358.
36. Asato, A. E., Watanabe, C., Li, X. Y. & Liu, R. S. H. (1992) *Tetrahedron Lett.* **33,** 3105–3108.
37. Weng, J., Mata, N. L., Azarian, S. M., Tzekov, R. T., Birch, D. G. & Travis, G. H. (1999) *Cell* **98,** 13–23.
38. Mata, N. L., Tzekov, R. T., Liu, X., Weng, J., Birch, D. G. & Travis, G. H. (2001) *Invest. Ophthalmol. Visual Sci.* **42,** 1685–1690.
39. Fishkin, N., Pescitelli, G., Sparrow, J. R., Nakanishi, K. & Berova, N. (2004) *Chirality* **16,** 637–641.
40. Duhamel, L., Guillemont, J., Poirier, J. M. & Chabardes, P. (1991) *Tetrahedron Lett.* **32,** 4495–4498.
41. Thomas, A. F. & Guntzdubini, R. (1976) *Helv. Chim. Acta* **59,** 2261–2267.
42. Lamb, T. D. & Pugh, E. N. (2004) *Prog. Ret. Eye Res.* **23,** 307–380.
43. Radu, R. A., Mata, N. L., Nusinowitz, S., Liu, X., Sieving, P. A. & Travis, G. H. (2003) *Proc. Natl. Acad. Sci. USA* **100,** 4742–4747.
44. Katz, M. L., Norberg, M. & Stientjes, H. J. (1992) *Invest. Ophthalmol. Visual Sci.* **33,** 2612–2618.
45. Sparrow, J. R. & Boulton, M. (2005) *Exp. Eye Res.*, in press.
46. Boulton, M., Rozanowska, M. & Rozanowski, B. (2001) *J. Photochem. Photobiol. B* **64,** 144–161.
47. Margrain, T. H., Boulton, M., Marshall, J. & Sliney, D. H. (2004) *Prog. Ret. Eye Res.* **23,** 523–531.
48. Ham, W. T., Ruffolo, J. J., Mueller, H. A., Clarke, A. M. & Moon, M. E. (1978) *Invest. Ophthalmol. Visual Sci.* **17,** 1029–1035.
49. Ham, W. T., Mueller, H. A., Ruffolo, J. J., Millen, J. E., Cleary, S. F., Guerry, R. K. & Guerry, D. (1984) *Curr. Eye Res.* **3,** 165–174.